Mechanical and electrical properties of stretched clean and H-contaminated Pd-nanowires

2008 Nanotechnology 19 335711

(http://iopscience.iop.org/0957-4484/19/33/335711)

Nanotechnology **19** (2008) 335711 (8pp) doi:10.1088/0957-4484/19/33/335711

Mechanical and electrical properties of stretched clean and H-contaminated Pd-nanowires

B Pieczyrak[1,2], C González[1,3], P Jelínek[3], R Pérez[1], J Ortega[1] and F Flores[1]

[1] Departamento de Física Teórica de la Materia Condensada, Universidad Autónoma de Madrid, E-28049, Spain
[2] Institute of Experimental Physics, University of Wroclaw, plac Maksa Borna 9, 50-204 Wroclaw, Poland
[3] Institute of Physics, Academy of Sciences of the Czech Republic, Cukrovarnická 10, 162 53, Prague, Czech Republic

E-mail: cesar.gonzalez@uam.es

Received 7 May 2008, in final form 9 June 2008
Published 8 July 2008
Online at stacks.iop.org/Nano/19/335711

Abstract
We analyze theoretically the formation of stretched Pd-nanowires and their interaction with hydrogen. In our approach, we simulate the nanowire stretching process using a first-principles molecular-dynamics method to obtain realistic atomic geometries of the contact in its final stages before the nanowire breaks. The electrical conductance of the nanowire is also calculated at each point of the deformation path. For the clean Pd-nanowire in the last stages of the deformation process we find that the nanowire develops, first, a one-atom-neck and, at the end, a dimer whose bond is finally broken. For these atomic configurations, the calculated electrical conductances are in good agreement with the experimental evidence. The interaction with hydrogen is analyzed adsorbing one or two H atoms on the Pd-nanowire for different configurations along the stretching process. In the case of one H atom we obtain geometries with conductances in the range 0.8–1.4G_0, while for two H atoms we find conductance plateaus with values $\sim$0.5G_0 and $\sim$1.0G_0. These results are in excellent agreement with the experimental evidence for nanocontact breaking in an H_2 atmosphere and indicate that the conductance peak around 0.5G_0 observed experimentally is associated with nanowires where two H atoms have been adsorbed.

(Some figures in this article are in colour only in the electronic version)

1. Introduction

Metallic nanowires [1] have been formed and analyzed using the scanning tunneling microscope [2] and mechanically controllable break junctions [3]. Their conductances, forces [4], and chemical properties are characteristic of the metal forming the contact. In particular, superconducting measurements have shown a close relationship between the chemical valence of the atom(s) forming the contact and the number of channels contributing to the transmission probabilities [5].

The interaction of hydrogen with those nanowires has been carefully studied for Au [6–9], Pt [10–12], and Pd [13–17]. For Au, the conductance changes due to hydrogen deposition suggest that stretched monoatomic chains are better catalysts than clean surfaces and that the interaction with the Au-nanowire probably breaks the H_2 molecule bond [8, 9]. For Pt, conductance measurements [10] suggest, however, that a single H_2 molecule forms a stable bridge between the Pt electrodes, contributing with a single channel to the measured conductance close to $1G_0$ ($G_0 = \frac{2e^2}{h}$ is the conductance quantum unit). For Pd, Csonka *et al* [13] have found an

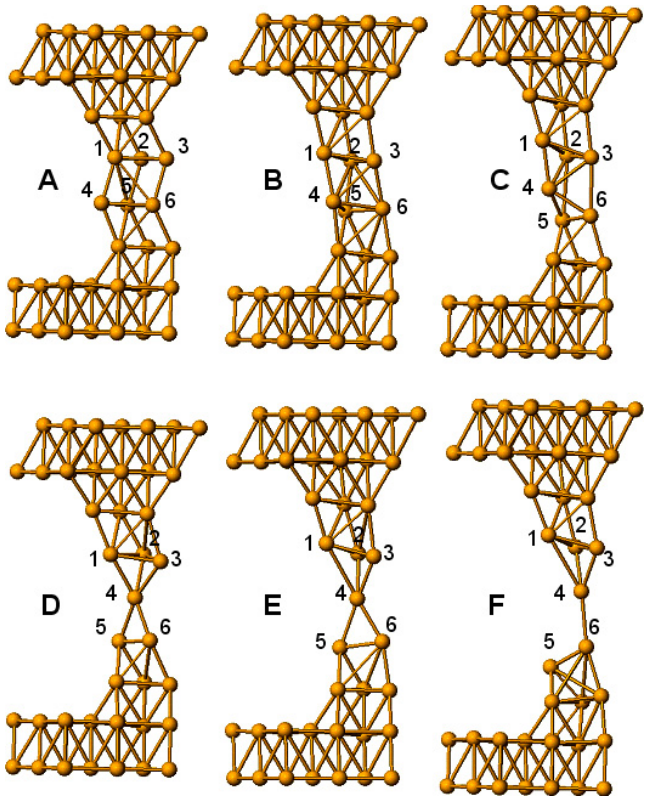

Figure 1. Atomic geometry of the clean Pd-nanowire along the stretching process. A–F illustrate different atomic configurations obtained in our calculations as a function of the stretching displacement (see also figure 2). The initial geometry is shown in snapshot A.

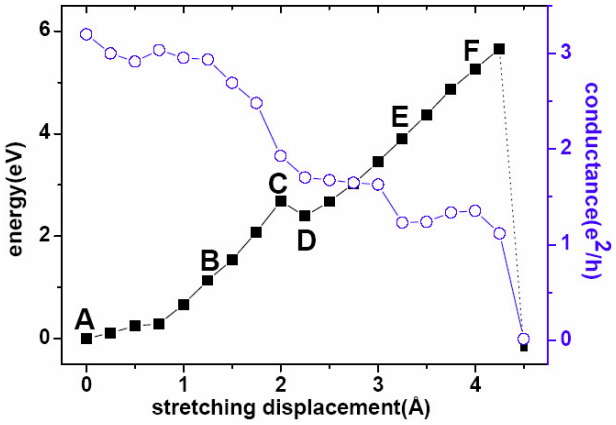

Figure 2. Total energy (squares) and conductance (circles) of the clean Pd-nanowire as a function of the stretching displacement. A–F indicate the position in this graph of the atomic geometries shown in figure 1. The dotted line at the end of the energy curve shows the abrupt drop of the energy when the nanowire is finally broken.

intermediate case. Similarly to the Pt case, clean Pd-nanowires do not form monoatomic chains in the last stages of the deformation process, but seem to react strongly with hydrogen, as in the Au case. At the same time, those authors have found important changes in the nanowire conductance upon hydrogen deposition: while for a clean contact, Pd (like Pt) shows a characteristic peak in the conductance histogram at $G = 1.7G_0$, in the presence of hydrogen this peak is replaced by two new peaks at around 0.5 and $1.0G_0$. Also, it is found that the $1.0G_0$ peak disappears when the amount of hydrogen is increased.

Theoretically, while the interaction of hydrogen with Au [7, 18–21, 8, 9] and Pt [11, 12, 15] nanowires has been analyzed by different authors, the case of Pd has received little attention [15, 16]. In this paper, we analyze theoretically the formation of Pd-nanowires upon stretching conditions and their interaction with hydrogen. At variance with other theoretical studies, in our approach we do not assume to know the final contact geometry but calculate it simulating the stretching process [22]. This procedure gives access to realistic atomic configurations for the nanowire in the final stages of the stretching process. The calculation of realistic atomic geometries for the nanowire is a key element of our analysis, allowing for an appropriate comparison with the experimental evidence. This approach has already been successfully used to analyze different Al- and Au-nanowires [22–24, 8, 9].

2. Model and method of calculation. Mechanical deformations and conductance of clean nanowires

Our simulations for stretched Pd-nanowires were performed using a very efficient first-principles (density functional theory-local density approximation, DFT-LDA) tight-binding molecular-dynamics technique (fireball) [25]. In these calculations we have used a basis set of $sp^3d^5d^{*5}$ (Pd) and ss^* (H) numerical atomic orbitals [26] using the following cutoff radii (in au): 4.8 (s), 5.6 (p), 4.5 (d) and 4.5 (d*) for Pd, and 3.8 (s), 3.8 (s*) for H. The electrical conductance of the Pd-nanocontacts was calculated, at each point of the deformation path, using a Keldysh–Green's function approach [23, 27] based on the first-principles tight-binding Hamiltonian [28] obtained from the local-orbital code.

We have analyzed the formation of a Pd-nanowire by stretching a thick Pd-wire having four layers, with three atoms each, sandwiched between two (111)-oriented metal electrodes (see figure 1(A)). We have used periodic boundary conditions along different directions: a 3×3-periodicity in the direction parallel to the (111)-surface, and, in the perpendicular direction, we have joined artificially the last layers of the two electrodes [22]: this amounts to using 48 atoms in our unit cell. The Brillouin zone was sampled using 16 special k-points. Starting from the atomic geometry shown in figure 1(A), we simulate the stretching of the system increasing the distance between the upper and lower layers in the unit cell in steps of 0.25 Å. After each 0.25 Å increase, the atomic positions are relaxed to the corresponding minimum energy configuration (excepting the atoms in the upper and lower layers, that are kept fixed). Figure 1 shows several atomic configurations obtained in this way for different stretching displacements, d (A: $d = 0$ Å, B: $d = 1.25$ Å, C: $d = 2.0$ Å, D: $d = 2.25$ Å, E: $d = 3.25$ Å, F: $d = 4.0$ Å). The total energy for the nanowire as a function of the stretching distance d is shown in figure 2.

In figure 1, configuration A shows the initial relaxed geometry with four layers in between the two electrodes (we take this case as the origin of the stretching distance d); in

configuration B, these four layers have been deformed to a straight geometry. In snapshot C, atom 4 has been displaced upwards, breaking its bond with the lower layer, approaching the layer of atoms 1–2–3 and moving above the two atoms 5–6. In configuration D, a new geometry with a narrow neck has developed, with atom 4 located in between the layer of atoms 1–2–3 and the dimer of atoms 5–6. In structure E, atom 1 has moved upwards and atom 5 downwards, in such a way that in configuration F a dimer is formed between atoms 4 and 6. This is the final structure defining the breaking geometry, since the nanowire breaks along this dimer (atoms 4–6). Notice the energy changes associated with the plastic deformations of the nanowire (figure 2): for instance, in the energy jump between configurations C and D, atom 4 has been reallocated to form the new structure D; in the same way, the energy kink between configurations A and B is associated with the new straightened structure found in snapshot B. In our calculations, the average length of the Pd–Pd bond in the center of figure 1(B) is around 2.5 Å, this length increasing with stretching in such a way that its value is around 2.85 Å when the bond is close to its breaking point (see figures 1(C) and (F), where bonds 3–6 and 4–6, respectively, are going to break). For comparison, we mention that in similar calculations for Au [8, 9], the mean Au–Au distance in the center of the neck is ∼2.6 Å, while the bonds break when their distance is close to 2.9 Å. These slight differences between Pd and Au are comparable to the different crystal bond lengths: 2.75 Å for Pd, and 2.89 Å for Au. It is also interesting to analyze the tensile forces appearing in both cases; for Pd, the wire initially suffers plastic deformations until reaching the straight geometry of figure 1(B); in the second stage of deformation the wire is deformed between $d = 0.75$ and 2.0 Å (see figure 2), with a force ∼3.2 nN; finally, between configurations D and F (figure 1), the force is around 2.6 nN. Comparison with Au can only be done directly for the first stages of deformation because for Au, after the nanowire reaches a geometry similar to figure 1(D), the system starts to develop an atomic chain of several atoms [8, 9]. In Au, in the initial stage of deformation, the maximum force is around 4 nN (a little larger than the value of 3.2 nN found for Pd), while along the stage of the atomic chain formation the force fluctuates around 2.5 nN, very similar to the force we find for Pd in the final stage for deformation (in Pd this process, however, mostly keeps a geometry having a neck of a single atom).

Figure 2 also shows the nanowire conductance as a function of the stretching displacement. Our calculations show three plateaus with conductances of $\sim 3G_0$, $\sim 1.75G_0$ and $\sim 1.35G_0$. The first plateau ($3G_0$) corresponds basically to the initial geometry with three atoms in the neck, while the second one ($1.75G_0$) corresponds to a geometry with a neck having one atom between two layers (figure 1(D)); the third one ($1.35G_0$) corresponds to the evolution from this geometry (with atoms 1 and 6 slightly displaced upwards, i.e. figure 1(E)) to the final dimer geometry (figure 1(F)). Comparing with the experimental conductance histograms of Csonka *et al* [13] we notice that, for clean Pd-nanowires, these authors also see a small peak around $3G_0$ and a broad peak around $1.7G_0$ (with a shoulder around $1.4G_0$). This broad peak can be associated with the two plateaus of $1.75G_0$ and $1.35G_0$ found in our calculations: in particular, we stress that along the deformation path from figure 1(D) to (E), the nanowire always keeps a very similar geometry with one atom located between two layers having three and two atoms. Only at the end of the stretching process does the system develop a dimer (similar to the one found in Al [22]), whose bond is broken in the final stage of the nanowire deformation (figure 1(F)).

3. Hydrogen adsorption on the stretched geometries

In this section, we consider the case of H adsorbed on different stretched Pd-nanowires. As a preliminary calculation, we have first examined H adsorption on a Pd(111)-surface. In these calculations, the surface was modeled by a slab with six Pd layers, using our theoretical equilibrium lattice parameter for bulk-Pd, 3.92 Å (experiment: 3.89 Å), and a 3×3 periodicity along the surface with 16 special k-points for surface Brillouin zone sampling. Figure 3 shows the density of states (DOS) for the Pd(111) clean surface and the H/Pd(111) system. For H/Pd(111) we have considered one H atom in the 3×3 unit cell (i.e. a coverage of 1/9 ML) adsorbed on a fcc position, which is the accepted most stable adsorption site [29–36]. The main effect of H adsorption on the DOS is the appearance of a localized surface state below the Pd conduction band, at ∼7.2 eV below the Fermi level E_F, associated with the H–Pd chemisorption bond. As shown in figure 3(a), this new DOS for the Pd atom is compensated by a small decrease in the DOS for energies near E_F. Figure 3(b) shows that both Pd sp-states and d-states present an equally important contribution in the H–Pd bonding state. These results for Pd(111) and H/Pd(111) are in good agreement with the DOS profiles obtained in previous DFT calculations [29, 33].

It is convenient to calculate the hydrogen adsorption energy E_a taking as reference the energy of the H_2 molecule:

$$E_a = E[\mathrm{H/Pd}] - E_R[\mathrm{Pd}] - \tfrac{1}{2}E[\mathrm{H_2}] \qquad (1)$$

where $E[\mathrm{H/Pd}]$ is the energy, per H atom, of the H/Pd system under consideration (i.e. an H atom adsorbed on the Pd-surface or Pd-nanowire), $E_R[\mathrm{Pd}]$ is the energy of the Pd reference system (i.e. without H atoms), and $E[\mathrm{H_2}]$ is the energy of the H_2 molecule. A negative value for E_a indicates that H adsorption is favored over the H_2 gas phase. In our calculations for the H/Pd(111) system mentioned above we obtain $E_a = -0.94$ eV and an equilibrium H–Pd distance of 1.85 Å. For comparison, other DFT calculations yield values in the range $E_a = -1.1 \pm 0.15$ eV (LDA) [29, 30, 36] or $E_a = -0.6 \pm 0.2$ eV (generalized gradient approximation, GGA) [33, 32, 31, 34, 35] depending on the exchange–correlation functional used (notice that we use the LDA functional). The experimental value is $E_a = -0.45$ eV [37] or, in other words, a binding energy of ∼2.8 eV for atomic hydrogen on Pd(111)[4]. Thus, our calculation for H on Pd(111) presents an overbinding of the order of ∼0.5 eV that has been shown to be mainly related to the LDA calculation for the H_2 molecule [29]. These calculations are expected to show

[4] Using a binding energy of 4.75 eV for the H_2 molecule.

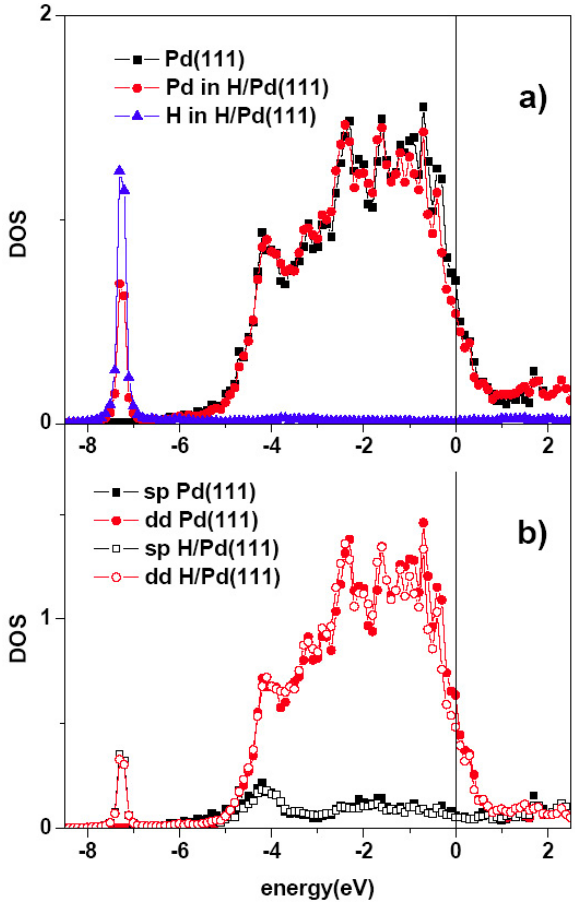

Figure 3. Density of states (DOS) for a Pd(111) clean surface and H/Pd(111) for an H-coverage of 1/9 ML on fcc sites. (a) Squares are the projected DOS on a surface Pd atom of clean Pd(111) while triangles represent the DOS on the H atom for the H/Pd(111) case and circles the DOS on a Pd atom bonded to the adsorbed H atom. (b) Projection on the sp (squares) and d (circles) orbitals of the Pd atoms.

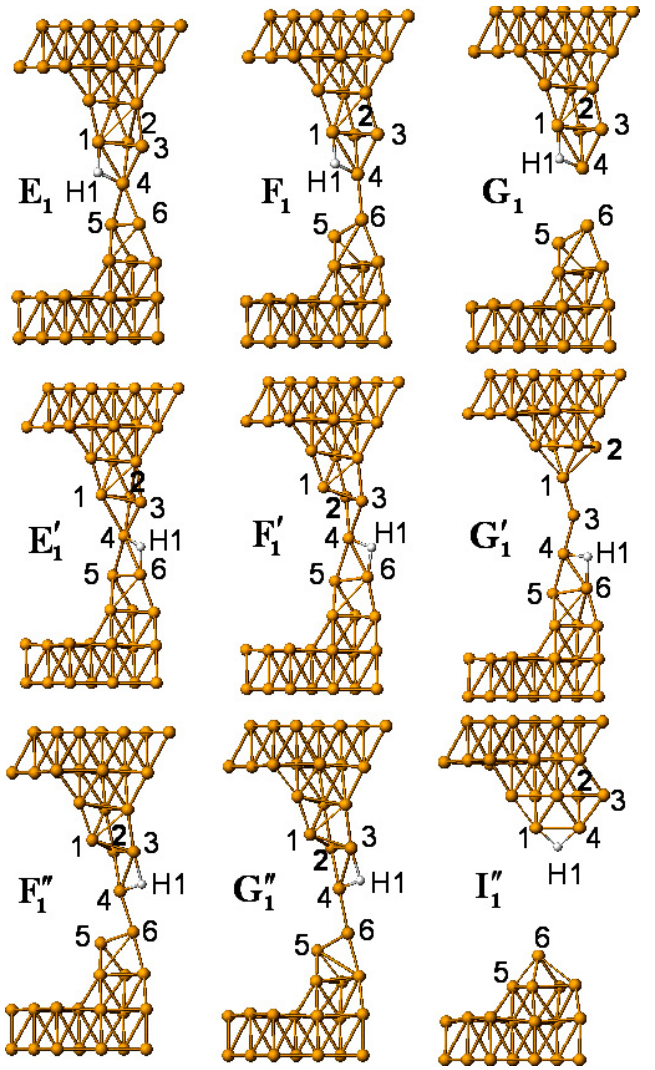

Figure 4. Atomic geometries for the adsorption of one H atom on the Pd-nanowire for three different cases. The initial configurations are shown in the first column. From these initial configurations the nanowire is stretched until it breaks. The second and third columns show snapshots of the evolution of the nanowire, as discussed in the text.

a much higher accuracy for energy differences between similar structures, such as the comparison between H adsorption on a Pd-surface and on a Pd-nanowire. In our calculations (see below) we obtain a similar E_a value for these two cases; since the H_2 molecule is highly reactive on Pd(111), we conclude that it should also dissociate on the Pd-nanowires discussed below.

The first column of figure 4 shows the initial geometries for the three different cases we have considered for one H atom adsorbed on the Pd-nanowire (labeled E_1, E'_1 and F''_1: initial letters refer to closely related configurations of the stretched nanowire in figure 1, and the subindex is related to the number of H atoms). In each case, the H atom is first placed at a given adsorption site on a particular geometry of the stretched Pd-nanowire (figure 1); from this initial configuration the system is further stretched, as explained above for the clean nanowire. In the first set of snapshots (figures 4E_1, F_1 and G_1), the H atom is placed in between Pd atoms 1 and 4 on a stretched nanowire geometry between configurations D and E in figure 1 (initial stretching displacement $d = 3.0$ Å, see figure 2); then, the system is stretched until it breaks. In our calculations, the H adsorption energy (relative to the H_2 molecule) for this case is $E_a = -0.62$ eV. Figures 4F_1 and G_1 show how the adsorbed H atom affects the geometry evolution of the stretched nanowire (mainly keeping the distance between atoms 1 and 4 practically constant). In particular, compare the geometries of figures 1(F) and 4F_1.

The sets of snapshots shown in figures 4E'_1, F'_1 and G'_1 correspond to the same initial stretched nanowire geometry, $d = 3.0$ Å, but different adsorption sites for the H atom. In this case, $E_a = -0.79$ eV, and the system evolves initially in a way similar to the clean nanowire case (compare figures 1(E) and 4F'_1). However, the evolution of this geometry in the final stage of deformation is completely different: due to the new H adsorption site, Pd atom 3 moves downwards and the nanowire develops a neck where this atom is located in between two pyramids, forming a trimer.

Snapshots shown in figures 4F''_1, G''_1 and I''_1 correspond to another geometry with H adsorbed initially on a configuration

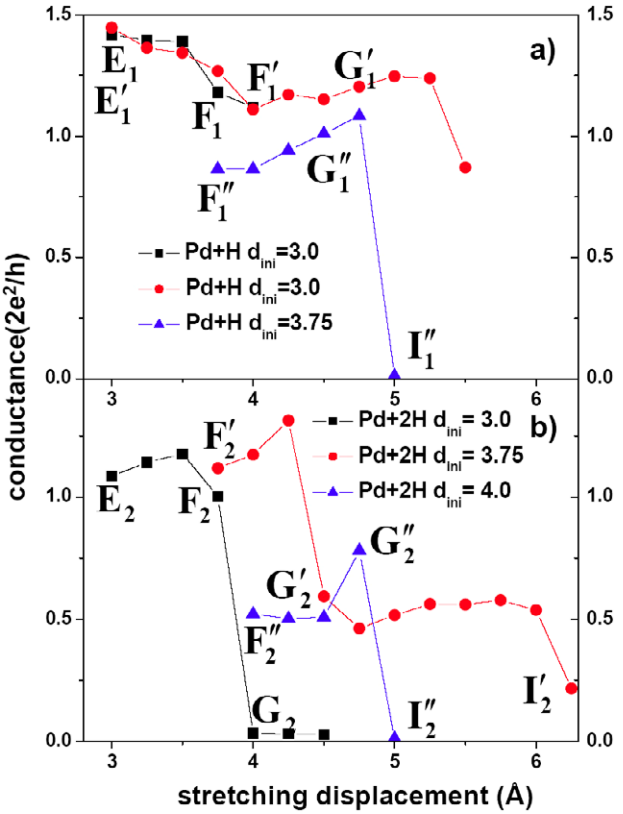

Figure 5. Evolution of the nanowire conductance as a function of the stretching displacement for (a) one H atom and (b) two H atoms adsorbed on the Pd-nanowire, see figures 4 and 6. The origin of the stretching displacement, d, is the same as in figure 2. Each figure contains three curves, corresponding to the three different initial geometries analyzed for each case. The labels in the graphs indicate the positions of the different geometries displayed in figures 4 and 6.

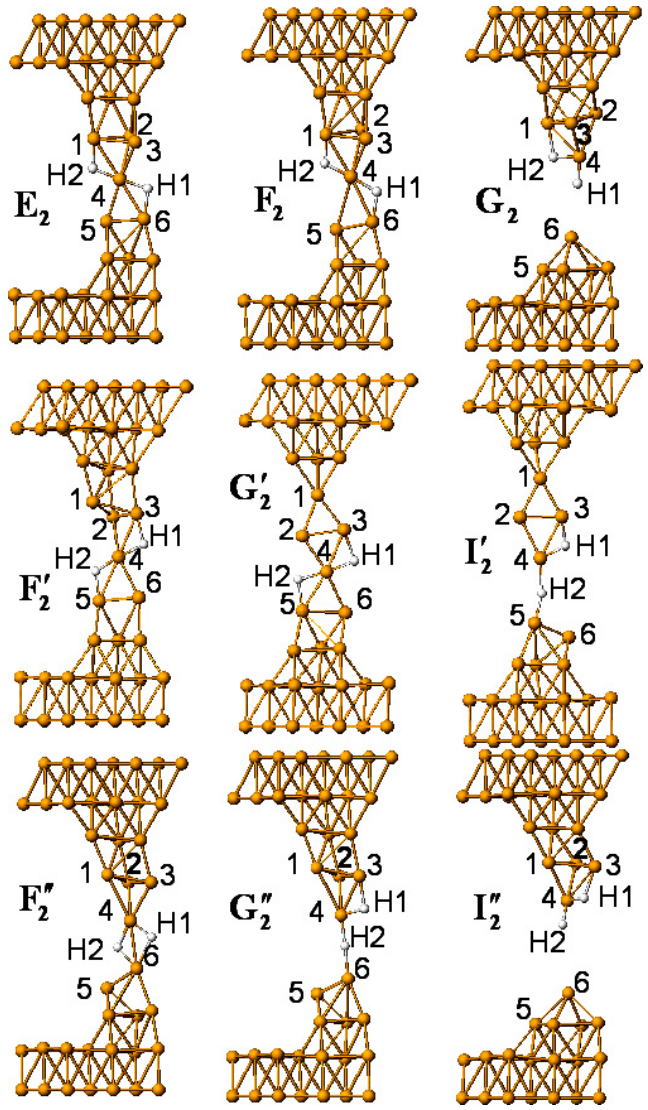

Figure 6. Atomic geometries for the adsorption of two H atoms on the Pd-nanowire for three different cases. The initial configurations are shown in the first column. From these initial configurations the nanowire is stretched until it breaks. The second and third columns show snapshots of the evolution of the nanowire, as discussed in the text.

close to that drawn in figure 1(F) ($d = 3.75$ Å). The H adsorption energy for this case is $E_a = -0.86$ eV, and the system evolves in a way quite similar to the case of figures 4E_1, F_1 and G_1, although there are some differences because in this case, before the nanowire breaks, the distance between atoms 3 and 4 remains practically constant due to the adsorbed H. We have also explored another initial geometry, starting with an H atom adsorbed between atoms 4 and 6 in figure 1(F). We find that the relaxed geometry for this case is practically the same as the geometry obtained in figure 4F'_1 starting from figure 4E'_1. The values of E_a obtained for the three cases of figure 4 are similar to the value obtained for the H/Pd(111)-surface, suggesting that the H_2 molecule should dissociate on the nanowire.

Figure 5(a) shows the evolution of the nanowire conductance as a function of the stretching displacement for the three cases discussed above (figure 4) for one hydrogen atom adsorbed on the nanowire. The conductance plateaus for these geometries are in the range 0.8–1.4G_0, which is in excellent agreement with a broad peak found by Csonka *et al* [13] around 1.0G_0 for Pd-nanowires in the presence of hydrogen, and not observed for the clean Pd-nanowire; this peak disappears when the amount of hydrogen in the experiments is increased. Another hydrogen-related peak at ∼0.5G_0 is observed in the same experiments, which does not disappear at high hydrogen concentrations. Thus, before analyzing the reason for the changes on the nanowire conductance due to the adsorption of H we first analyze the case of two H atoms adsorbed on the nanowire.

Figure 6 (first column) shows the three different initial atomic geometries we have analyzed with two H atoms adsorbed on the stretched nanowire (we use the same labeling scheme as for figure 4: initial letters refer to closely related configurations of the stretched nanowire in figure 1, and the subscript is related to the number of H atoms). The hydrogen adsorption energies E_a, relative to the H_2 molecule (see equation (1)) for these cases are: figure 6E_2 (initial geometry, $d = 3.0$ Å) $E_a = -0.72$ eV; figure 6F'_2 (initial geometry, $d = 3.75$ Å) $E_a = -0.53$ eV; figure 6F''_2 (initial geometry, $d = 4.0$ Å) $E_a = -0.83$ eV. These values show that the two

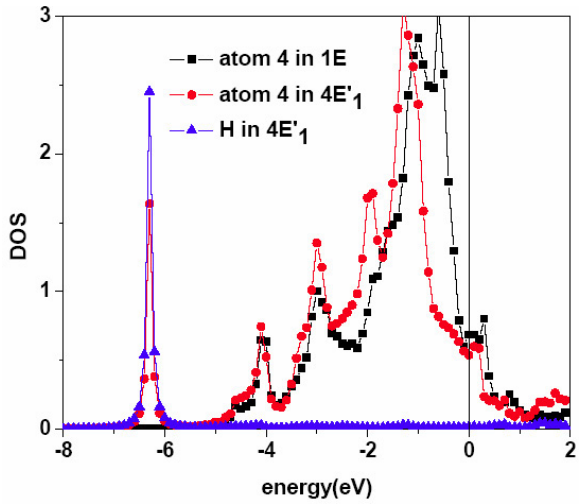

Figure 7. Density of states for one H atom adsorbed on the Pd-nanowire (figure 4E_1') and corresponding clean nanowire (figure 1(E)). Squares represent the projected DOS on a surface Pd atom in the center of the clean nanowire (atom 4 in figure 1(E)), while circles are the DOS on the corresponding Pd atom in figure 4E_1' and triangles the DOS on the H atom.

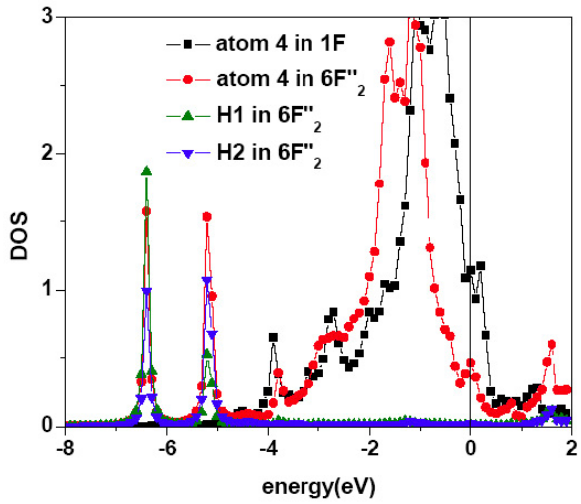

Figure 8. Density of states for two H atoms adsorbed on the Pd-nanowire (figure 6F_2'') and the corresponding clean nanowire (figure 1(F)). Squares are the projected DOS on a surface Pd atom in the center of the clean nanowire (atom 4 in figure 1(F)), while circles represent the DOS on the corresponding Pd atom in figure 6F_2'' and triangles the DOS on the H atoms.

hydrogen atoms adsorbed at the neck of the nanowire form strong bonds with the nanowire, with E_a energies similar to those found above for one hydrogen atom adsorbed on the Pd-nanowire.

The different stretched geometries shown in figure 6 present two cases with a similar evolution: in geometries 6E_2, 6F_2, and 6G_2, as well as in geometries 6F_2'', 6G_2'', and 6I_2'', the system evolves inserting one H atom between the Pd atoms forming the dimer (4–6), just before the nanowire breaks. In geometries 6F_2', 6G_2', and 6I_2', atoms 2, 3, 4, 5, 6, H1 and H2 are initially rather rigid due to the Pd–H bonds and atom 1 is displaced upwards to form a narrow neck between atoms 2–3 and a pyramid above; however, the nanowire breaks along the dimer 4–5 after atom H2 is inserted in this dimer.

Figure 5(b) displays the evolution of the conductance as a function of the stretching displacement for these three cases with two H atoms on the nanowire. The calculated conductances present two characteristic plateaus close to $1.0G_0$ and to $0.5G_0$; this last conductance value appears for the configurations found at the intermediate stage of the stretching process starting at 6F_2', and for the initial geometries of the process, starting at the configuration 6F_2''. These results are in very good agreement with the first peaks in the experimental histogram of Csonka *et al* [13], and suggest that two atomic hydrogens are probably adsorbed on the Pd-nanowire in geometries similar to those shown in figures 6F_2'' and G_2'.

In order to understand the reason behind the change found in the nanowire conductance upon H adsorption, we analyze the influence of the adsorbed hydrogen atoms on the electronic structure of the Pd-nanowires. Figure 7 shows the DOS for the central Pd atom at the neck of the nanowire (atom 4), for the cases shown in figure 4E_1' (one hydrogen atom adsorbed on the nanowire) and figure 1(E) (corresponding to a clean nanowire). As compared to the Pd(111) surface, the nanowire DOS shows a narrower conduction band, and a shift of the d-band towards E_F; when H is adsorbed on the nanowire, the Pd-DOS is shifted towards higher binding energies, and the DOS at E_F is slightly reduced. The Pd–H bonding state is now at ~ -6.3 eV below E_F.

Figure 8 shows a similar comparison for the case of two H atoms adsorbed on the nanowire, plotting the DOS for the case shown in figure 6F_2'' (two hydrogen atoms and $0.5G_0$ conductance) and for the case of figure 1(F) (the corresponding clean nanowire). Now we observe two Pd–H bonding states, as correspond to the two H atoms adsorbed on the nanowire; the DOS for each of these states presents a significant contribution from both H atoms, showing some interaction between them. The DOS at E_F for the central Pd atom at the neck of the nanowire is now significantly reduced, to less than half the value for the clean nanowire, due to the strong bonding interaction with the two hydrogen atoms adsorbed at the neck of the nanowire. This decrease in the DOS at the Fermi level is associated with the decrease in the electrical conductance: for the two hydrogen case of figure 6F_2'' the conductance is $\sim 0.5G_0$, with two conduction channels with transmissions 0.37 and 0.13, while for the other three cases (the clean nanowires of figures 1(E), (F) and the one hydrogen atom case of figure 4E_1') we obtain $G \sim 1.4G_0$ with three main conduction channels with transmissions $\sim$0.9, $\sim$0.35, and $\sim$0.15. For comparison, the structures with conductance $G \sim 1G_0$ (e.g. figures 4F_1'', F_1', or 6E_2) present two main channels with transmissions $\sim$0.8 and $\sim$0.2.

Thus, we find that the changes due to H-contamination on the nanowire conductance are mainly related to the decrease, induced by the adsorbed H atoms, on the DOS at the Fermi level for the Pd atom at the neck of the nanowire. This point is further analyzed in figures 9 and 10, which compare

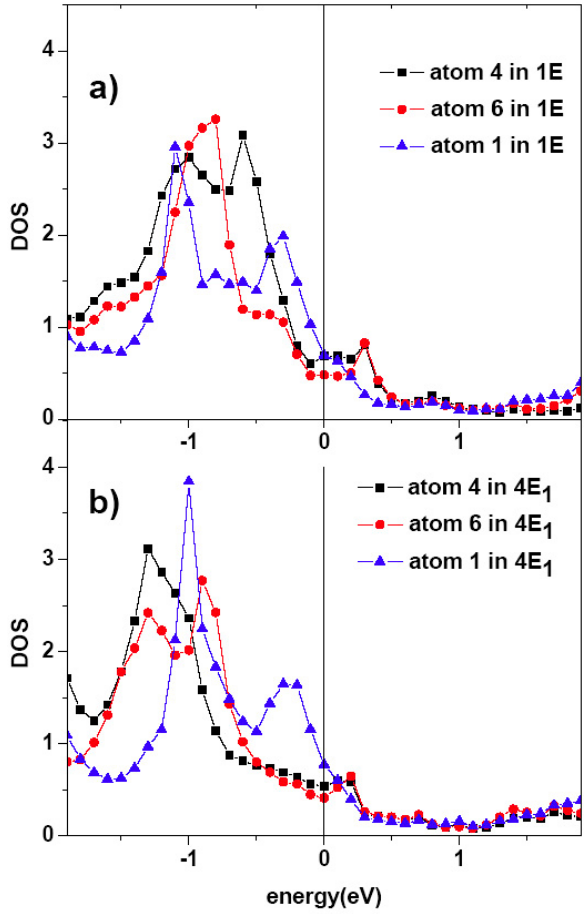

Figure 9. Density of states at three different Pd atoms in the neck of the nanowire (atoms 1, 4, 6 in figures 1(E) and 4E$'_1$) around the Fermi level (0 eV): (a) clean nanowire (figure 1(E)); (b) one hydrogen adsorbed on the nanowire (figure 4E$'_1$).

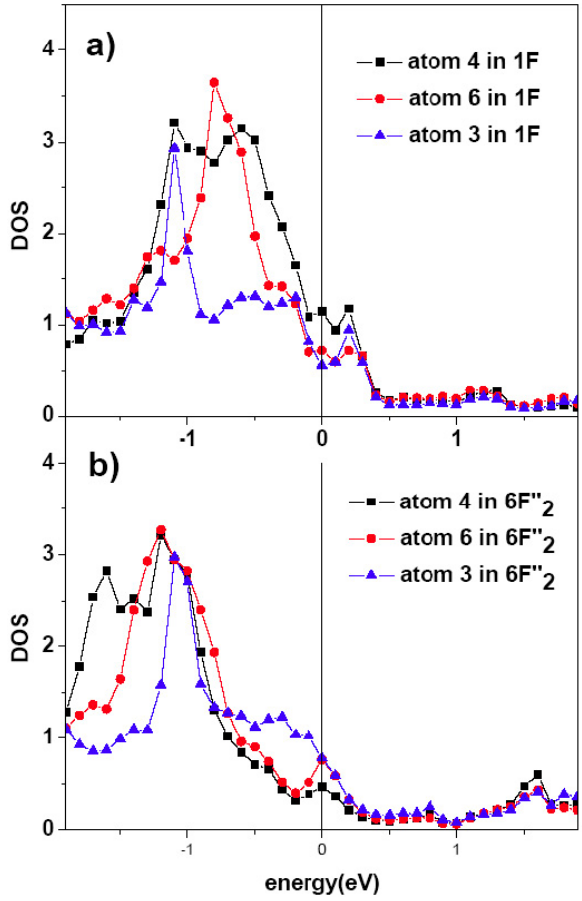

Figure 10. Density of states at three different Pd atoms in the neck of the nanowire (atoms 3, 4, 6 in figures 1(F) and 6F$''_2$) around the Fermi level (0 eV): (a) clean nanowire (figure 1(F)); (b) two hydrogen atoms adsorbed on the nanowire (figure 6F$''_2$).

the DOS close to E_F for three Pd atoms at the neck of the nanowire. As shown in these figures, while for one H atom on the nanowire no big changes are observed for the DOS at E_F, a significant reduction at the central Pd (atom 4) is clearly seen in figure 10(b) when two hydrogen atoms are adsorbed on the nanowire; for this case the conductance changes from $\sim 1.4G_0$ for the clean nanowire (figure 1(F)) to $\sim 0.5G_0$ (figure 6F$''_2$). For Pt-nanowires, García *et al* [14] have analyzed a similar Pt–H configuration, obtaining also a reduction in the conductance of the order of $1G_0$ (from $G \sim 2G_0$ to $G \sim 1G_0$). The different value obtained in this case for the conductance ($G \sim 1G_0$) as compared with our 6F$''_2$ case ($G \sim 0.5G_0$) is probably due to the different atomic geometries: while in [14] a simplified symmetric geometry was assumed, figure 6F$''_2$ represents a more realistic geometry obtained after a complex relaxation process.

The observation of the $G \sim 0.5G_0$ peak in the experimental conductance histograms for Pd-nanowires in a hydrogen environment was originally explained as due to dissolved hydrogen on the Pd electrodes [13]; our calculations offer an alternative explanation, in which this peak is related to nanowire configurations with two hydrogen atoms adsorbed close to the neck. These hydrogen atoms induce a decrease in DOS at E_F for the central Pd atom at the neck, which is responsible for the decrease in the conductance.

Finally, it is interesting to make a comparison with the case of H adsorbed on Au-nanowires. In [8, 9] we have applied a similar methodology to analyze the formation of Au-nanowires under stretching, and their interaction with hydrogen. This system presents two important differences: (a) contrary to the H/Pd case, H adsorption on the Au-surface is not favored with respect to H_2 molecules (i.e. $E_a > 0$; we obtain [9] $E_a = +0.76$ eV); (b) Au-nanowires form monoatomic chains in the last stages of the deformation process, but this is not the case for Pd-nanowires. In our calculations we obtain for H/Pd a similar hydrogen adsorption energy on the surface or on the nanowire, $E_a \sim -0.9$ eV, showing that H adsorption is in both cases clearly favored with respect to H_2 molecules. For the H/Au system, while H_2 does not dissociate on the surface, for the nanowire we find an increasingly negative value for E_a as the number of Au atoms on the monoatomic Au chain is increased: $E_a \sim -0.3$, -0.6 and -1.0 eV for two, three and four Au atoms on the chain. This difference between Au and Pd has been analyzed in terms of the position of the d-band relative to E_F [33]. For the Au-surface, the d-band is well below E_F and is completely filled; for the Au-nanowires the reduced dimensionality as well as the strain move the d-band close to

E_F, increasing the chemical reactivity (i.e. making E_a more negative) [8, 9]. On the other hand, for the Pd-surface the d-band is already close to E_F and is partially filled (see figure 3). Therefore the surface is already very reactive ($E_a < 0$), and the narrowing and shift of the d-band in the Pd-nanowires do not decrease further the value of E_a.

4. Conclusions

We have analyzed the formation of stretched Pd-nanowires and their interaction with hydrogen using first-principles techniques. Instead of assuming ideal geometries for the nanowire, we search for realistic atomic geometries simulating the stretching process by means of an efficient local-orbital DFT-LDA molecular-dynamics technique. For each point of the deformation path the electrical conductance of the nanowire is calculated via a Keldysh–Green's function formalism using the first-principles tight-binding Hamiltonian obtained from the local-orbital calculation. This approach is applied to the cases of clean Pd-nanowire as well as to Pd-nanowires with one or two adsorbed H atoms. For the clean nanowire case we obtain atomic geometries that are characterized by the formation of a one-atom-neck (see figures 1(D) and (E)) just before the formation of a dimer (figure 1(F)) where the contact is finally broken. For these geometries we obtain conductance plateaus around $\sim$1.75 and $\sim 1.35G_0$ that can be associated with the broad peak at $\sim 1.7G_0$ (with a shoulder at $\sim 1.4G_0$) observed experimentally by Csonka *et al* [13]. When H atoms are adsorbed on the nanowire we obtain atomic geometries (see figures 4 and 6) that yield conductances around $1G_0$ for one H atom (figure 5(a)), while for two H atoms geometries with conductances $\sim 0.5G_0$ and $\sim 1.0G_0$ are obtained. This is in excellent agreement with the experimental results [13] that show peaks at $\sim 0.5G_0$ and $\sim 1.0G_0$ in the conductance histograms for Pd-nanowires in the presence of hydrogen. In our calculations the $0.5G_0$ peak is related to nanowire configurations with two adsorbed hydrogen atoms; these atoms induce a decrease in the DOS at E_F for the Pd atom at the neck of the nanowire, reducing the nanowire conductance to $\sim 0.5G_0$.

Acknowledgments

This work has been supported by the DGI-MCyT (Spain) under contracts MAT2004-01271, MAT2005-01298, MAT2007-60966, and NAN2004-09183-C10-07, and by the Comunidad de Madrid under contract 0505/MAT-0303. PJ acknowledges the financial support from COST P19 (OC150); the Institutional Research Plan no. AV0Z10100521 and GAAV under the grants Nos KAN400100701, IAA100100616 and IAA1010413. CG acknowledges the financial support by the Spanish Ministerio de Educacion y Ciencia under grant No. -2007-0034.

References

[1] Agräit N, Levy-Yeyati A and van Ruitenbeek J 2003 *Phys. Rep.* **377** 81
[2] Rubio G, Agräit N and Vieira S 1996 *Phys. Rev. Lett.* **76** 2302
[3] Scheer E, Joyez P, Esteve D, Urbina C and Devoret M H 1997 *Phys. Rev. Lett.* **78** 3535
[4] Rubio-Bollinger G, Bahn S R, Agräit N, Jacobsen K W and Vieira S 2001 *Phys. Rev. Lett.* **87** 026101
[5] Scheer E, Agrait N, Cuevas J C, Levy Yeyati A, Ludoph B, Martín-Rodero A, Bollinger G R, van Ruitenbeek J M and Urbina C 1998 *Nature* **394** 154
[6] Csonka S, Halbritter A, Mihály G, Jurdik E, Shklyarevskii O I, Speller S and van Kempen H 2003 *Phys. Rev. Lett.* **90** 116803
[7] Barnett R N, Hakkinen H, Scherbakov A G and Landman U 2004 *Nano Lett.* **4** 1845
[8] Jelinek P, Pérez R, Ortega J and Flores F 2006 *Phys. Rev. Lett.* **96** 046803
[9] Jelinek P, Pérez R, Ortega J and Flores F 2008 *Phys. Rev.* B **77** 115447
[10] Smit R H M, Noat Y, Untiedt C, Lang N D, van Hermert M C and Ruitenbeek J M 2002 *Nature* **419** 906
[11] Cuevas J C, Heurich J, Pauly F, Wenzel W and Schön G 2003 *Nanotechnology* **14** 29
[12] Thygesen K S and Jacobsen K W 2005 *Phys. Rev. Lett.* **94** 036807
[13] Csonka S, Halbritter A, Mihály G, Shklyarevskii O I, Speller S and van Kempen H 2004 *Phys. Rev. Lett.* **93** 016802
[14] García Y, Palacios J J, SanFabián E, Vergés J A, Pérez-Jiménez A J and Louis E 2004 *Phys. Rev.* B **69** 041402(R)
[15] García-Suárez V M, Rocha A R, Bailey S W, Lambert C J, Sanvito S and Ferrer J 2005 *Phys. Rev.* B **72** 045437
[16] Wu X, Li Q and Yang J 2005 *Phys. Rev.* B **72** 115438
[17] Kiguchi M, Miura S, Hara K, Sawamura M and Murakoshi K 2006 *Appl. Phys. Lett.* **88** 253112
[18] Bahn S R, Lopez N, Norskov J K and Jacobsen K W 2002 *Phys. Rev.* B **66** 081405(R)
[19] Novaes F D, da Silva A J R, da Silva E Z and Fazzio A 2003 *Phys. Rev. Lett.* **90** 036101
[20] Legoas S B, Galväo D S, Rodrigues V and Ugarte D 2002 *Phys. Rev. Lett.* **88** 076105
[21] Anglada E, Torres J A, Yndurain F and Soler J M 2007 *Phys. Rev. Lett.* **98** 096102
[22] Jelinek P, Pérez R, Ortega J and Flores F 2003 *Phys. Rev.* B **68** 085403
[23] Jelinek P, Pérez R, Ortega J and Flores F 2004 *Surf. Sci.* **566–568** 13–23
[24] Jelinek P, Pérez R, Ortega J and Flores F 2005 *Nanotechnology* **16** 1023
[25] Jelinek P, Wang H, Lewis J P, Sankey O F and Ortega J 2005 *Phys. Rev.* B **71** 235101
Lewis J P, Glaesemann K R, Voth G A, Fritsch J, Demkov A A, Ortega J and Sankey O F 2001 *Phys. Rev.* B **64** 195103
Demkov A A, Ortega J, Sankey O F and Grumbach M P 1995 *Phys. Rev.* B **52** 1618
[26] Sankey O F and Niklewski D J 1989 *Phys. Rev.* B **40** 3979
Basanta M A, Dappe Y J, Jelinek P and Ortega J 2007 *Comput. Mater. Sci.* **39** 759
[27] Mingo N, Jurczyszyn L, Garcia-Vidal F J, Saiz-Pardo R, de Andres P L, Flores F, Wu S Y and More W 1996 *Phys. Rev.* B **54** 2225
[28] Ortega J 1998 *Comput. Mater. Sci.* **12** 192
[29] Dong W, Kresse G, Furthmüller J and Hafner J 1996 *Phys. Rev.* B **54** 2157
[30] Paul J F and Sautet P 1996 *Phys. Rev.* B **53** 8015
[31] Dong W and Hafner J 1997 *Phys. Rev.* B **56** 15396
[32] Lovvik O M and Olsen R A 1998 *Phys. Rev.* B **58** 10890
[33] Pallassana V, Neurock M, Hansen L B, Hammer B and Norskov J K 1999 *Phys. Rev.* B **60** 6146
[34] López N, Lodziana Z, Illas F and Salmeron M 2004 *Phys. Rev. Lett.* **93** 146103
[35] Hong S and Rahman T S 2007 *Phys. Rev.* B **75** 155405
[36] Kim S, Kim S-K and Erwin S C 2007 *Phys. Rev.* B **76** 214109
[37] Conrad H, Ertl G and Latta E E 1974 *Surf. Sci. Lett.* **41** 435